Redox Biology 46 (2021) 102078

Contents lists available at ScienceDirect

Redox Biology

journal homepage: www.elsevier.com/locate/redox

An ACE2/Mas-related receptor MrgE axis in dopaminergic neuron mitochondria

Rita Valenzuela [a,b,**], Ana I. Rodriguez-Perez [a,b], Maria A. Costa-Besada [a,c], Rafael Rivas-Santisteban [b,d], Pablo Garrido-Gil [a,b], Andrea Lopez-Lopez [a], Gemma Navarro [b,e], Jose L. Lanciego [b,f], Rafael Franco [b,d], Jose L. Labandeira-Garcia [a,b,*]

[a] Cellular and Molecular Neurobiology of Parkinson's Disease, Research Center for Molecular Medicine and Chronic Diseases (CIMUS), IDIS, University of Santiago de Compostela, Santiago de Compostela; Spain
[b] Networking Research Center on Neurodegenerative Diseases (CIBERNED), Spain
[c] Cell and Developmental Biology Department, University College London, London, UK
[d] Laboratory of Molecular Neurobiology, Department of Biochemistry and Molecular Biology, Faculty of Biology, University of Barcelona, Barcelona, Spain
[e] Department of Biochemistry and Physiology, Faculty of Pharmacy, University of Barcelona, Barcelona, Spain
[f] Neuroscience Department, Center for Applied Medical Research (CIMA, IdiSNA), University of Navarra, Pamplona, Spain

ARTICLE INFO

Keywords:
Alamandine
Angiotensin 1-7
Angiotensin converting enzyme 2
Parkinson
Oxidative stress
Renin-angiotensin system

ABSTRACT

ACE2 plays a pivotal role in the balance between the pro-oxidative pro-inflammatory and the anti-oxidative anti-inflammatory arms of the renin-angiotensin system. Furthermore, ACE2 is the entry receptor for SARS-CoV-2. Clarification of ACE2-related mechanisms is crucial for the understanding of COVID-19 and other oxidative stress and inflammation-related processes. In rat and monkey brain, we discovered that the intracellular ACE2 and its products Ang 1–7 and alamandine are highly concentrated in the mitochondria and bind to a new mitochondrial Mas-related receptor MrgE (MrgE) to produce nitric oxide. We found MrgE expressed in neurons and glia of rodents and primates in the substantia nigra and different brain regions. In the mitochondria, ACE2 and MrgE expressions decreased and NOX4 increased with aging. This new ACE2/MrgE/NO axis may play a major role in mitochondrial regulation of oxidative stress in neurons, and possibly other cells. Therefore, dysregulation of the mitochondrial ACE2/MrgE/NO axis may play a major role in neurodegenerative processes of dopaminergic neurons, where mitochondrial dysfunction and oxidative stress play a crucial role. Since ACE2 binds SARS-CoV-2 spike protein, the mitochondrial ACE2/MrgE/NO axis may also play a role in SARS-CoV-2 cellular effects.

1. Introduction

The renin-angiotensin system (RAS) was initially considered an endocrine system mainly related to regulation of blood pressure and sodium homeostasis. However, local or paracrine RAS were identified in different tissues and organs, including brain, and intracellular or intracrine RAS have been observed in different cell types [1–4]. At these three levels, RAS shows a prooxidative proinflammatory axis, which is counteracted by an antioxidative anti-inflammatory axis. A number of physiological functions are the result of an adequate equilibrium between both axes, and its disruption is involved in pathological processes. Major components of the prooxidative axis are angiotensin converting enzyme (ACE), which produces angiotensin II (Ang II) that acts on Ang II type 1 receptors (AT1). Major components of the counterregulatory antioxidative arm are Ang II acting on Ang II type 2 receptors (AT2) and, particularly, ACE2, which mainly produces Ang 1–7 that is the endogenous ligand of the Mas receptor (MasR). Previous studies have shown that brain RAS deregulation is involved in neuroinflammation and neurodegeneration, and we have shown the involvement of brain RAS, both at paracrine [5–7] and intracellular/intracrine [8–10] levels, in dopaminergic oxidative stress and neuron degeneration

* Corresponding author. Research Center for Molecular Medicine and Chronic diseases (CIMUS), University of Santiago de Compostela, 15782 Santiago de Compostela, Spain.
** Corresponding author. Research Center for Molecular Medicine and Chronic diseases (CIMUS), University of Santiago de Compostela, 15782 Santiago de Compostela, Spain.
E-mail addresses: rita.valenzuela@usc.es (R. Valenzuela), joseluis.labandeira@usc.es (J.L. Labandeira-Garcia).

https://doi.org/10.1016/j.redox.2021.102078
Received 24 March 2021; Received in revised form 17 July 2021; Accepted 19 July 2021
Available online 22 July 2021

Abbreviations:

ACE2	Angiotensin converting enzyme 2
ala	Alamandine
Ang 1–7	Angiotensin 1-7
Ang II	Angiotensin II
AT1	Ang II type 1 receptors
AT2	Ang II type 2 receptors
CD11b	Cluster of differentiation molecule 11b
Ct	Cycle threshold
DIC	differential interference contrast
DMEM	Dulbecco's modified Eagle's medium
D-Pro	D-Proline
FAM-Alamandine	Fluorophore-conjugated alamandine
FC	frontal cortex
FRET	fluorescence resonance energy transfer
GFAP	Glial fibrillary acidic protein
GPCRs	G-protein–coupled receptors
LCM	Laser capture microdissection
MasR	Mas receptors
MrgE	Mas-related G-protein coupled receptor member E
MRGPR	Mas related receptor family
mRNA	Messenger RNA
MTDR	Mitotracker Deep Red probe
NO	Nitric oxide
NOX4	NADPH oxidase 4
OC	Occipital cortex
PB	Phosphate buffer
PD	Parkinson's disease
RAS	Renin-angiotensin system
SN	Substantia nigra
ST	Striatum
TH	Tyrosine hydroxylase
VDAC	Voltage-dependent anion channel
VM	Ventral mesencephalon
WB	Western blot

in Parkinson's disease (PD) models.

Interestingly, it is now known that ACE2, a key component of the antioxidant anti-inflammatory RAS axis, is also the entry receptor used by SARS-CoV-2 to invade cells [11,12], and a virus-induced dysregulation of the ACE2 and, subsequently, RAS function plays a major role in the inflammatory and fibrotic processes observed in COVID-19 disease in several organs. Although lung lesions are particularly dangerous, other organs are also affected, including brain [13–15]. Possible effects of this type of viruses on dopaminergic neuron death and PD have also been suggested [16,17]. Clarification of the role of ACE2, particularly within the cell, is crucial and remains unclear. In dopaminergic neurons, we have previously observed AT1, AT2 and Mas receptors at the mitochondrial level, which modulate the mitochondrial function and oxidative stress [8,9]. Surprisingly, we observed that intracellular ACE2 was highly concentrated in the mitochondrial fraction as compared with the whole cell homogenate, and mitochondria also had high levels of its product Ang 1–7, suggesting a major role of the mitochondria in ACE2-related intracellular effects. In contrast, the major receptor for Ang 1–7 (i.e. MasR) was at relatively low levels in the mitochondria in comparison with whole cell homogenates [8], suggesting that other receptors mediate the effects of the ACE2/Ang 1–7 on the mitochondrial function. We investigated the Mas related receptor family (MRGPR), which is a group of receptors identified in rodents and humans. Six MRG genes, MrgD, MrgE, MrgF, MrgG, MrgH and Mas1, were observed in rodents, with clear human orthologs [18,19]. Almost all are considered "orphan" receptors. MrgD subtype is the best known and characterized member, and it was related to the natural MasR ligand, angiotensin 1-7 (Ang 1–7) [20], and to the now considered RAS component alamandine (Ala), a heptapeptide structurally similar to Ang 1–7 [21]. The aim of this study, mainly focused on dopaminergic neurons, was to figure out the mechanism that mediates the effects of the ACE2-induced peptides Ang 1–7 and alamandine in the mitochondria and particularly, major mitochondrial receptors responsible for their effects.

2. Materials and methods

2.1. Experimental design

In previous studies, we found relatively low expression of MasR in the mitochondrial fraction in comparison with mitochondrial ACE2 and Ang 1–7 levels [8].Therefore, in a first set of experiments, we investigated the presence of possible additional unknown receptors which may bind Ang 1–7 in the mitochondria. First, we investigated the expression of major Mas related receptors (i.e. MrgD, MrgE and MrgF) in cell homogenates of substantia nigra compared to nigral MasR and a control tissue with already known levels of Mas related receptors (i.e. testis) using RT quantitative PCR and Western blot (WB) analyses. As MrgE was the most abundant Mas related receptor, we isolated mitochondria from the rat nigral region to investigate the possible presence of mitochondrial MrgE using WB for MrgE, mitochondrial marker voltage-dependent anion channel (VDAC) as a marker for mitochondrial fraction, and α-tubulin and GAPDH as markers for cytosol fractions. The specificity of the used ACE2 and MrgE antibodies was assessed in our laboratory by WB analysis of lysates from HEK293 cells transiently transfected with MrgE tagged to fusion tail DDK and ACE2-GFP respectively. Colocalization of MrgE and mitochondrial markers (MTDR) in dopaminergic neurons was confirmed by double immunolabeling and confocal microscopy in cultures of N27 dopaminergic neurons.

Then, we investigated by RT-PCR and WB whether MrgE was the most abundant Mas related receptor only in the SN or was also located in other brain areas (striatum, frontal and occipital cortex). In order to identify the cell types showing MrgE receptors, we first used primary mesencephalic cultures and brain sections through the SN, which were analyzed by double immunolabeling for MrgE and the neuronal marker NeuN, the dopaminergic neuron marker tyrosine hydroxylase (TH), the astrocytic marker glial fibrillary acidic protein (GFAP), and the microglial marker CD11b (complement receptor-3, clone MRC OX42). Then, we used laser capture microdissection (LCM) and RT-PCR of isolated neurons and glial cells from the SN and striatum to further confirm the specificity of the MrgE antibody and that MrgE transcripts are located in neurons and glial cells. Finally, major results observed in rats were confirmed in non-human primate (*Macaca fascicularis*) SN using double immunofluorescence and confocal microscopy for MrgE and different markers of neurons and glial cells, and WB of isolated mitochondria.

A second set of experiments were designed to study functional effects of brain MrgE receptors. First, we performed fluorescence competition binding studies in MrgE and Mas receptor transfected HEK293 cells to find out the ligands of MrgE receptors. As possible ligands we tested the ACE2-derived products Ang 1–7 (MasR ligand) and Alamandine (MrgD ligand), and also the MrgD ligand β-Alanine, in the presence/absence of the MrgD blocker D-Proline (D-Pro) or the MasR blocker A-779. Subsequently, cells were incubated with fluorescence labeled alamandine (FAM-alamandine). To verify whether the binding of the ACE2-derived peptides alamandine and/or Ang 1–7 to MrgE produces a functional response in cells, we evaluated levels of nitric oxide (NO) release using live-cell fluorescence time-lapse assays and a DAF-FM Diacetate fluorescent probe in HEK293 cells transfected with MrgE receptor or an empty plasmid as a control. Finally, we investigated the functionality of

mitochondrial MrgE receptors. First, we used pure isolated brain mitochondria to exclude any interference of effects of cellular non-mitochondrial receptors. Mitochondrial NO production was detected with a NO fluorometric assay kit. Then, we confirmed MrgE-derived mitochondrial NO production using confocal microscopy and a NO fluorescence probe DAF-FM diacetate in MTDR labeled mitochondria of HEK293 cells transfected with MrgE receptor. We investigated the increase in mitochondrial NO production after treatment with alamandine and/or Ang 1–7. We also observed basal or constitutive mitochondrial NO production in N27 dopaminergic neurons using colocalization of the NO fluorescence probe DAF-FM diacetate with MTDR labeled mitochondria by confocal microscopy.

In a third set of experiments, we studied possible dysregulation of the mitochondrial MrgE/ACE2 axis by aging. The effect of aging in tissue and mitochondrial MrgE expression was studied using cell homogenates of rat substantia nigra and pure brain isolated mitochondria from young adult (2–3-month old) and aged (18–20-month old) male rats using RT-PCR and WB analysis. In addition, aging related changes in protein expression of mitochondrial ACE2 and the intracellular NADPH form NOX4 were investigated.

2.2. Cell cultures

Mesencephalic primary cultures were obtained by dissecting ventral mesencephalic tissues from rat embryos of 14 days of gestation (E14). After an incubation of 20 min at 37 °C with 0.1 % of trypsine, 0.05% of DNase (Sigma), and DMEM (Invitrogen), the tissue was washed and mechanically dissociated in DNase/DMEM. The cell suspension was centrifuged at 50×*g* for 5 min, and the resulting pellet was resuspended in 0.05 % DNase/DMEM. Cells were plated at a density of 1.5×10^5 cells/cm^2 onto 35-mm culture dishes (Falcon) previously coated with poly-L-lysine (100 μg/ml; Sigma) and laminin (4 μg/ml; Sigma), and maintained under control conditions (DMEM/HAMS F12/(1:1) containing 10 % fetal bovine serum (FBS) in a humidified CO_2 incubator (5 % CO_2; 37 °C) for 8 days in vitro (DIV); the entire culture medium was removed on day 2 and replaced with a fresh culture medium.

The dopaminergic cell line N27 (SCC048, Millipore, MA, USA) was cultured in RPMI 1640 medium supplemented with 10 % FBS, 2 mM L-glutamine (Sigma), 100 U/ml penicillin, and 100 μg/ml streptomycin. Human embryonic kidney 293 cells, HEK293 (CRL-11268, ATCC), were cultured in DMEM medium supplemented with 10 % FBS, 2 mM L-glutamine (Sigma), 100 U/ml penicillin, and 100 μg/ml streptomycin.

2.3. Animal models

Tissue from SN of young (2–3-month old) and aged (18–20-month old) Sprague-Dawley male rats were used for immunolabeling, WB and RT-PCR. Non-human primate tissue from six adult (4.5–5-year old) male *Macaca fascicularis* was used for confirming major results in rat tissue. Animal handling was conducted in accordance with the Directive 2010/63/EU, European Council Directive 86/609/EEC and the Spanish legislation (RD53/2013). For monkeys, the experimental design was approved by the Ethical Committee for Animal Testing of the University of Navarra (ref: 009–12). Monkeys were captive-bred and supplied by R. C. Hartelust (Leiden, The Netherlands). Rodent experiments were approved by the corresponding committee at the University of Santiago de Compostela. Animals were housed at constant room temperature (RT) (21–22 °C) and 12-h light/dark cycle.

2.4. Isolation of mitochondria from rat and monkey ventral midbrain and cell cultures

Mitochondria from ventral midbrain of rat and monkey were isolated and purified according to the protocol described by Sims and Anderson [22] with few modifications [9]. This protocol was performed to isolate pure mitochondria with minimum contamination by synaptosomes and myelin, and combines differential centrifugation and discontinuous Percoll density gradient centrifugation. Ventral midbrain was removed and rinsed in cold isolation buffer (0.32 M sucrose, 1 mM and 10 mM TRIS; pH 7.4). The tissue was cut into small pieces, transferred to a Dounce homogenizer with 12 % Percoll solution, and then homogenized on ice using a loose-fitting and tight-fitting glass pestles. The homogenate was slowly layered on a previously prepared discontinuous Percoll gradient consisting of 26 % Percoll layered over 40 % Percoll and centrifuged using a fixed-angle rotor at 30 700×*g* for 5 min at 4 °C. Three separate bands were produced during centrifugation, and the enriched mitochondrial fraction, which was located at the interface between the 26 and 40 % Percoll layers, was carefully taken out with a glass Pasteur pipette. The mitochondrial fraction was diluted with isolation buffer and was centrifuged at 16 700×*g* for 10 min at 4 °C. This provided a mitochondrial pellet, which was softly resuspended in the residual supernatant. Finally, the pellet was resuspended in isolation buffer and centrifuged at 7300×*g* for 10 min at 4 °C, producing a pellet of pure mitochondria that was used for WB. The same procedure was performed with rat whole-brain tissue to measure mitochondrial NO production.

2.5. Western blot analysis

Isolated mitochondria from rat and monkey ventral midbrain, homogenates from rat different brain regions and rat testicle were lysed in RIPA buffer containing PMSF (Sigma) and protease inhibitor cocktail (Sigma). Tissue lysates were centrifuged and total proteins were quantified using the Pierce BCA Protein Assay Kit (Thermo Scientific). An equal amount of protein lysates were separated on a 10 % Bis-Tris polyacrylamide gel and transferred to nitrocellulose membranes. Membranes were incubated overnight at 4 °C with primary antibodies against the MrgE receptor (TA316024; Origene; 1:750), ACE2 (ab108252; Abcam; 1:1.000) and NOX4 (ab133303; Abcam; 1:800). Membranes were reincubated with loading controls: anti-α-tubulin (T5168; 1:50.000; Sigma), GAPDH (G9545; 1:25.000; Sigma) and β-actine (A2228; Sigma, 1:10.000) as markers of whole homogenate, anti-VDAC/porin (V2139; Sigma; 1:1.000) as a marker of mitochondrial fraction. The following horseradish peroxidase (HRP)-conjugated secondary antibodies were used: goat anti-rabbit-HRP and goat anti-mouse-HRP Santa Cruz Biotechnology; 1:2.500). Bound antibody was detected with an Immun-Star HRP Chemiluminescent Kit (Bio-Rad; 170–5044) and visualized with a chemiluminescence detection system (Bio-Rad; Molecular Imager ChemiDoc XRS System). The data were then expressed relative to the value obtained for the control to counteract possible variability among batches.

2.6. RNA extraction and real-time quantitative polymerase chain reaction

Total RNA from rat different brain regions and testicle was extracted with TRIzol (Invitrogen, Paisley, UK) following the manufacturer's protocol. Total RNA (2 μg) was reversed transcribed to complementary DNA (cDNA) using nucleoside triphosphate containing deoxyribose, random primers and Moloney murine leukaemia virus (M-MLV; Invitrogen, Thermo Fisher Scientific; 200U) reverse transcriptase. Subsequently, the RT-PCR analysis was performed with a QuantStudio 3 platform (Applied Biosystems, Foster City, CA, USA), the EvaGreen qPCR MasterMix (Applied Biological Materials Inc., Vancouver, Canada), and primer sequences indicated below were used to examine the relative levels of Mas, MrgD, MrgE and MrgF receptors. β-Actin was used as a housekeeping gene and was amplified in parallel with the genes of interest. We used the comparative cycle threshold values (cycle threshold (Ct)) method ($2^{-\Delta\Delta Ct}$) to examine the relative messenger RNA (mRNA) expression. A normalized value was obtained by subtracting the Ct of β-actin from the Ct of interest (ΔCt). As it is uncommon to use ΔCt as a relative expression data due to this logarithmic characteristic, the $2^{-\Delta\Delta Ct}$ parameter was used to express the relative expression data.

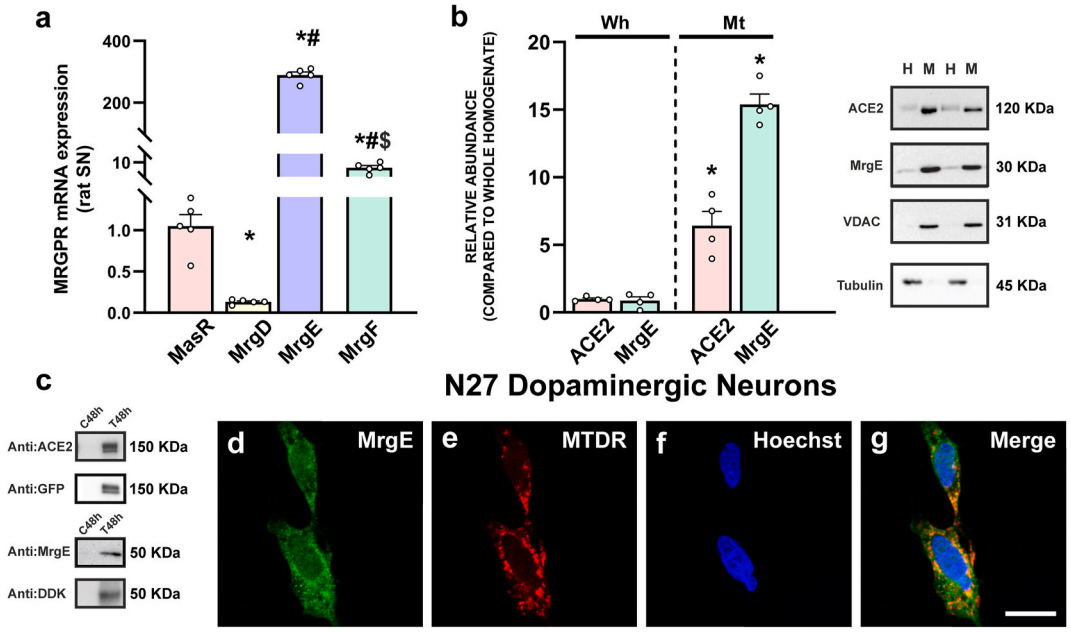

Fig. 1. ACE2 and MrgE receptors in the rat substantia nigra (SN) and cultured dopaminergic neurons. (a) In the SN, MrgE mRNA expression was much higher than Mas receptor and other Mrg receptor expression. **(b)** In isolated mitochondria from the nigral region, ACE2 and MrgE receptors (together with the mitochondrial marker VDAC) were highly concentrated, as compared with the whole cell homogenate (identified by the cytosol marker tubulin). **(c)** The specificity of ACE2 and MrgE antibodies was confirmed by Western blot analysis of HEK293 cells transfected with ACE2-GFP or MrgE-DDK, which showed a predominant immunoreactive band compared to control non-transfected cells at 48 h post-transfection. **(d-g)** In dopaminergic N27 cells, MrgE labelling was predominantly cytoplasmatic and colocalized with MTDR-positive mitochondrial labelling. Data are presented as mean ± s.e.m. *$p < 0.05$, Kruskal-Wallis One Way Analysis of Variance on Ranks with Student-Newman-Keuls Method post hoc test (a); Student's *t*-test (MrgE) and Mann-Whitney Rank Sum Test (ACE2) (b). Scale bar = 25 μm. Abbreviations: ACE2, Angiotensin Converting Enzyme 2; H or Wh, whole homogenate; MasR, Mas Receptor; M or Mt, Mitochondrial fraction; MrgE, Mas-related G-protein coupled receptor member E; MrgD, Mas-related G-protein coupled receptor member D; MrgF, Mas-related G-protein coupled receptor member F; MTDR, MitoTracker Deep Red; VDAC, Voltage-dependent anion-selective channel 1. (For interpretation of the references to colour in this figure legend, the reader is referred to the Web version of this article.)

Primer sequences were as follows: for Mas receptors, forward 5′-CTTTGTGGAGAACGGGAT-3′, reverse 5′-GGAGATGTCAGCAATGGA-3′; for MrgD, forward 5′-CTGTGACCTGGGTTTACTTT-3′, reverse 5′-CTCAGTAGCCAAATCACCAT-3'; for MrgE, forward 5′-GCCTGAT-CATGCTGCGGTTC-3′, reverse 5′-AGCAGCAGGTCCAGTAGCAG-3'; for MrgF, forward 5′-CTCTGCGAAGGGAACTCGGA-3′, reverse 5′-GAGTC-CAGGCTCCTGTTGGG-3'; and for β-actin, forward 5′-TCGTGCGTGA-CATTAAAGAG-3′ and reverse 5′-TGCCACAGGATTCCATACC-3'.

2.7. Immunofluorescence labelling

Mesencephalic primary cultures were grown on glass coverslips and co-incubated overnight at 4 °C with different cell markers and a rabbit polyclonal MrgE receptor antibody (LS-C136078, LSBio, 1:100). Different cell types were identified with the corresponding mouse monoclonal antibodies: anti-NeuN (Millipore, 1:500) as neuronal marker, anti-TH (Sigma; 1:5.000) as dopaminergic marker, anti-glial fibrillary acidic protein (GFAP, Millipore, 1:500) as astrocyte marker, or anti-CD11b (complement receptor-3, clone MRC OX42, Serotec; 1:100) as microglial marker. Primary antibodies were diluted in DPBS containing 1 % BSA and 2 % normal donkey serum. Then, the following fluorescent secondary antibodies were incubated for 2 h at RT: Alexa Fluor 568- conjugated donkey anti-rabbit IgG (Molecular Probes; 1:200) or Alexa Fluor 488-conjugated donkey anti-mouse IgG (Molecular Probes; 1:200).

In other experiments, mitochondria from N27 dopaminergic cells were marked with the cell-permeant Mitotracker Deep Red probe (MTDR) (M-22426; InvitroGene; 200 nM) for 15 min and fixed with 4 % paraformaldehyde. After mitochondrial labelling, neurons were incubated with MrgE receptor antibody (LS-C136078, LSBio, 1:100) overnight, followed by the secondary antibody Alexa Fluor 488- conjugated donkey anti-rabbit IgG (Molecular Probes; 1:200). Cell nuclei were marked with the DNA-binding dye Hoechst 33 342 (Sigma; 10 μg/ml) for 30 min at RT. Finally, mounting was performed with Immumount (Thermo-Shandon).

Rats and monkeys were sacrificed with an overdose of chloral hydrate and transcardially perfused with a cold 4 % paraformaldehyde solution in phosphate buffer (PB). Then, brain was removed, cryoprotected and cut into coronal tissue sections (40-μm thick) using a sliding microtome. Tissue sections through the entire SN were processed for double immunofluorescence to identify cells expressing MrgE receptor. The antibody against MrgE receptor was combined with antibodies against tyrosine hydroxylase (TH) as dopaminergic marker, or glial fibrillary acidic protein (GFAP) as astrocytic marker or cluster of differentiation molecule 11b (CD11b) as microglial marker. Free-floating SN sections were pre-incubated in KPBS-1% BSA with 5 % normal donkey serum (Sigma) and 0.05 % Triton X-100 (60 min at RT). Tissue sections were then incubated overnight at 4 °C in primary antibodies raised against MrgE receptor (1:100; rabbit polyclonal, LS-C136078, LSBio) and TH (1:1000; mouse monoclonal, T2928, Sigma) or GFAP (1:500; mouse monoclonal; MAB360, Millipore) or rat CD11b (1:50; mouse monoclonal clone OX-42, MCA275, BioRad) or CD11b (1:50; goat polyclonal, Santa Cruz Biotechnology) diluted in KPBS-1% BSA with 5 % normal donkey serum. Immunoreactivity was visualized with the following fluorescent secondary antibodies from Molecular Probes (diluted 1:200): Alexa Fluor 568- conjugated donkey anti-rabbit IgG, Alexa Fluor 488-conjugated donkey anti-mouse IgG, and Alexa Fluor 488-conjugated donkey anti-goat IgG. Finally, SN sections were mounted on gelatin-coated slides and coverslipped with Immumount (Thermo-Shandon). Co-localization of markers was confirmed by confocal laser microscopy (AOBS-SP5X; Leica Microsystems Heidelberg GmbH, Mannheim, Germany) performing sequential scan to avoid any

potential overlap with the LAS AF software (Leica Microsystems GmbH).

2.8. Transfection of MrgE receptor

HEK293 cells were seeded at a density of 0.4×10^6/well onto 24 well plates with or without glass cover depending on the post-analysis and maintained at 37 °C in a humidified CO_2 incubator (5 % CO_2, 95% air). Cells were transiently transfected with 1 μg of MrgE cDNA (MRGE Myc DDK-tagged, MR216310, Origene) using a commercial transfection reagent, Turbofect (R0533, Thermo Scientific). After a period of 48 h post-transfection, cells were lysed with RIPA and immunoblotted for antibody specificity testing, directly used for in vivo time lapse experiments, or fixed for confocal studies.

For binding studies, HEK293 cells were transiently transfected with the corresponding cDNA using the PEI (PolyEthylenImine, Sigma-Aldrich, St. Louis, MO) method. Briefly, the cDNA diluted in 150 mM NaCl was mixed, 10 min, with PEI (5.5 mM in nitrogen residues) prepared in 150 mM NaCl. cDNA-PEI complexes were transferred to HEK293 cell cultures (6-weel plates) and incubated for 4 h in a serum-free Dulbecco's modified Eagle's medium (DMEM). Then, the medium was substituted by 10 % fetal-calf-serum supplemented DMEM and cells were maintained at 37 °C in a humid atmosphere of 5 % CO_2. Experiments were done 48 h after transfection.

2.9. Specifity of ACE2 and MrgE antibodies and ACE2 activity

The specificity of the MrgE antibody (TA316024, Origene) and ACE2 antibody (ab108252, Abcam) was assessed in our laboratory by WB analysis of lysates from HEK293 cells transiently transfected with MrgE tagged to fusion tail DDK and ACE2-GFP respectively. The specificity was confirmed by the presence of a predominant immunoreactive band in positively transfected lysates, after 48 post-transfection of MrgE receptor (TA316024, Origene; 1:750) or ACE2 enzyme (ab108252, Abcam, 1:1.000) and the absence of the fusion tail DDK (TA50011; Origene; 1:1.000) band or mouse monoclonal turboGFP antibody (TA150041; Origene; 1:1.000) in negative controls (see Fig. 1 c).

ACE2 activity of the mitochondrial fraction from rat and monkey brain was measured using a commercial ACE2 activity assay kit (AnaSpec, AS-72086) following the manufacturer's specifications. The kit is based on the Mca/Dnp fluorescence resonance energy transfer (FRET) peptide (10 μM). In the FRET peptide, the fluorescence of Mca is quenched by Dnp but a cleavage of the substrate produces a separation into two fragments by the enzyme, so that the fluorescence of Mca is measured at excitation/emission = 330/390 nm using an Infinite M200 multiwell plate reader (TECAN). ACE2 activity was confirmed with the specific ACE2 inhibitor DX600 1 μM, included as a control in the same kit (AnaSpec, AS-72086).

2.10. Laser capture microdisection of rat neurons and glial cells

Rat tissue sections containing the SN or striatum were stained with a shortened protocol for neutral red (1 %; 2 min on ice). LCM was performed using a PALM MicroBeam (Zeiss) system controlled by PALM Robo software. Nigral and striatal neurons and glial cells were visualized under bright-field microscopy at 40x magnification (see for details our previous methodological publication [23]). Cell pools (1000 nigral or striatal neurons or glial cells per animal; n = 4) were selected using the corresponding software, and then cut and catapulted by laser pulses into an adhesive microtube cap (Zeiss). Cell pools were immediately lysed for 30 min at RT in lysis buffer (RNeasy Microkit, Qiagen) and stored at −80 °C until RNA extraction. Then the samples of isolated neurons or glia were processed for MrgE RT-PCR as described above. The PCR products were loaded into a 2 % agarose gel with Syber Safe (Invitrogen), separated by electrophoresis and visualized with an UV detection system (Molecular Imager Chemidoc XRS System, BioRad).

2.11. Fluorescence competition binding studies in MrgE-transfected HEK293 cells

To perform non-radioactive fluorescent ligand binding assays, binding of fluorophore-conjugated alamandine (FAM-alamandine) was tested in control cells and transfected cells expressing Mas-related E (Mrgpre,1 μg cDNA) or Mas (MAS1, 1 μg cDNA) G-protein–coupled receptors (GPCRs). Cells were carefully washed twice with phosphate-buffered saline (PBS, pH 7.4). Then cells were incubated for 10 min with the following non-fluorescent compounds: the Mas ligands Ang 1–7 (10 μM) and Alamandine (10 μM), the MrgD ligand β-Alanine (10 μM), the Mas receptor antagonist A779 (10 μM) or the MrgD antagonist D-Proline (10 μM). Then, cells were incubated with fluorescence labeled alamandine (FAM-alamandine; 0,1 μM). Incubation was kept for 1 h, light-protected and at room temperature. Cells were then washed twice with PBS, detached and distributed in 96-well microplates (black plates with a transparent bottom). Fluorescence measurements were performed by VICTOR Multilabel Plate Reader (PerkinElmer) using a 10 nm bandwidth 495 nm excitation filter and a 10 nm bandwidth 519 nm emission filter. Imaging of FAM-Alamandine fluorophore labeled cells were performed by ZOE Fluorescent Cell Imager (Bio-Rad) inverted microscope equipped with a 20X objective. Brightfield channel uses a ring of multiple green LEDs to avoid chromatic aberration. Green channel for fluorescence images uses a blue LED which is compatible with FAM fluorophore labeled alamandine (excitation and emission wavelength 480/517 nm).

2.12. Live-cell fluorescence time-lapse assays

To determine the production of cellular NO due to activation of MrgE receptors, a DAF-FM Diacetate fluorescent probe (D-23844, ThermoFisher Scientifics) was used in HEK293 cells transfected with MrgE receptor and an empty plasmid as a control. HEK293 cells were seeded in 24-well plate at a density of 3×10^4 cells/well, and transfected with MrgE or empty plasmid. Forty-eight hours after transfection, cells were incubated for 30 min at RT with the DAF-FM Diacetate probe (5 μM), and washed to remove the excess of probe. Treatments with alamandine (1 μM) or Ang 1–7 (1 μM) were added directly under the microscope, and time-lapse differential interference contrast (DIC) images and fluorescence at 495 and 515 nm (3 fields/well) were captured using a 20X objective at 2 min intervals for the following 30 min. Image capture was achieved automatically, using a Cell Observer instrument (LEICA CTR 7000 HS) equipped with a cell incubation chamber, motorized stage, CCD camera. All operations were under the control of the Software Leica LAS X. The same conditions of laser intensities/exposure times were used for the entire experiment.

2.13. Mitochondrial nitric oxide production

Mitochondrial nitric oxide (NO) production was detected with a NO fluorometric assay kit (Biovision) in pure isolated mitochondria from rat brain. Total concentrations of nitrates and nitrites have been used as indicators of NO production. Direct quantification of NO is complex due to its brief half-time. An amount of 30 μg of brain isolated mitochondria was incubated for 10 min with MrgD inhibitor, D-Pro (5 μM) and/or 5 min with alamandine (1 μM) to investigate the effect of mitochondrial MrgE receptor activation. Then all nitrates were turned into nitrites by nitrate reductase enzyme. Finally, nitrite reacted with the fluorescent probe DAN (2,3-diaminonaphthalene) and the measurement of nitrite concentration was used as a quantitative measure of NO production. Fluorescence was measured in an Infinite M200 multiwell plate reader (TECAN).

Basal mitochondrial NO production of dopaminergic neurons or MrgE-derived mitochondrial production in MrgE transfected HEK-293T cells were detected by quantifying the NO fluorescence probe DAF-FM Diacetate (InvitroGene, D-23844) in labeled mitochondria. Cells were

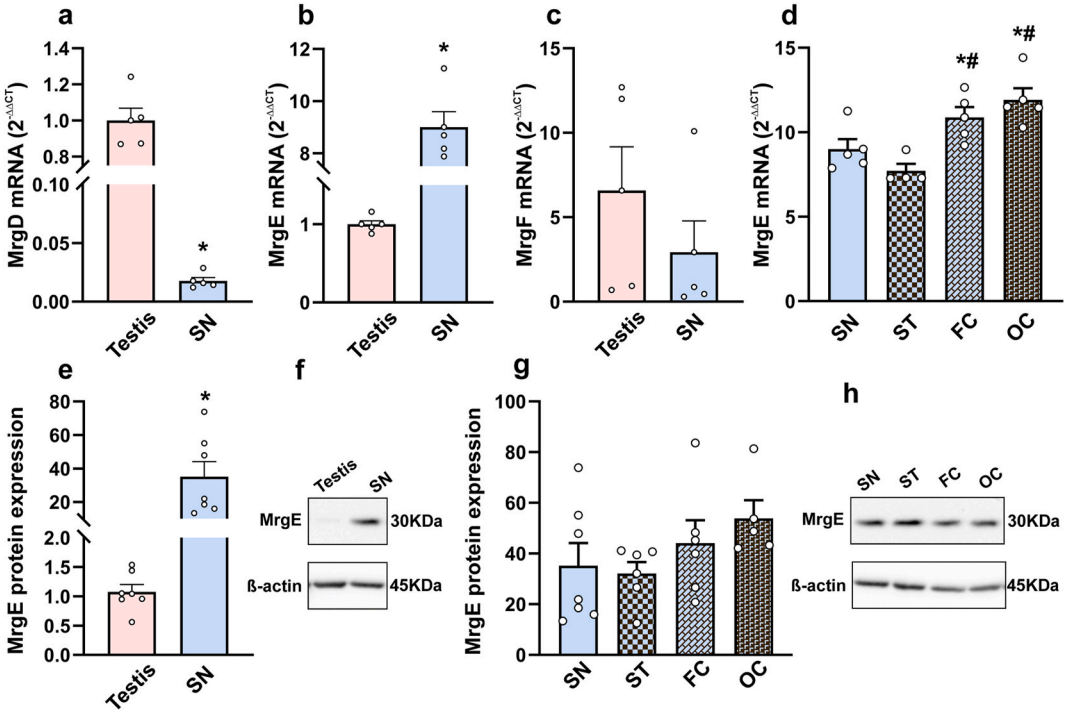

Fig. 2. Major Mas related receptors (MrgD, MrgE and MrgF) in different brain regions. (**a-h)** Expression of mRNA and protein of major Mas-related receptors in cell homogenates from testis (positive control for MrgD), substantia nigra (SN) and other areas of the brain (striatum, frontal cortex, occipital cortex; ST, FC, OC). Data are presented as mean ± s.e.m. *p < 0.05, Mann-Whitney Rank Sum Test (**a, b, e**); Student's *t*-test (**c**); One Way Anova (**d, g**) with Student-Newman-Keuls method post hoc test (**d**). Abbreviations: MrgE, Mas-related G-protein coupled receptor member E; MrgD, Mas-related G-protein coupled receptor member D; MrgF, Mas-related G-protein coupled receptor member F.

seeded at 12-well plates (5×10^4 cells/well). Then, the DAF-FM probe (5 μM) was incubated for 30 min. During the last 20 min of loading the NO probe, a mitochondrial marker (Mitotracker deep red, MTDR; 200 nM) was added to the cells for 10 min. Then, cells were washed and treated or not treated with alamandine (1 μM) or Ang 1–7 (1 μM) to assess the NO production. Cells were fixed and co-localization of DAF-FM and MTDR was confirmed by confocal laser microscopy (AOBS-SP5X; Leica Microsystems Heidelberg GmbH, Mannheim, Germany) performing sequential scan to avoid any potential overlap with the LAS AF software (Leica Microsystems GmbH). Quantification of fluorescence intensity was done with the open-source image processing package based on ImageJ software (NIH, Bethesda, MD, USA, rsb.info.nih.gov/ij/).

2.14. Statistical analysis

All statistical analyses were performed using SigmaPlot 11.0 (Systat Software, Inc., CA, USA). All datasets were tested for normality with the Kolmogorov–Smirnov test. If the dataset passed the normality test, parametric tests were used: Student's *t*-test for two group comparisons and one-way ANOVA followed by the Student-Newman-Keuls Method for multiple comparisons. For non-parametric data, two group comparisons were carried out by Mann-Whitney Rank Sum Test and multiple comparisons by Kruskal-Wallis One Way Analysis of Variance on Ranks test followed by Student-Newman-Keuls Method or Dunn's Method. Differences were considered statistically significant at $p < 0.05$. No statistical methods were used to predetermine sample sizes, but our sample sizes were similar to those reported previously [7–10,24].

3. Results

3.1. Discovery of MrgE as a mitochondrial receptor

In previous studies we found relatively low expression of Mas receptors in the mitochondrial fraction in comparison with the whole cell homogenate. However, ACE2 concentration was much higher in mitochondrial fraction than in the whole cell homogenate [8], suggesting a major role of this enzyme in mitochondria. Furthermore, we observed that Ang 1–7 is more abundant than Ang II in pure isolated mitochondria from rat nigral region, suggesting an important role for Ang 1–7 in the mitochondrial function and that it may act not only via mitochondrial Mas receptors but also via additional unknown receptors.

To identify possible mediators of the Ang 1–7 action, first we investigated the expression of major Mas related receptors (MrgD, MrgE and MrgF) in cell homogenates of substantia nigra. Surprisingly, we observed that MrgD mRNA, which is the best-studied Mas related receptor, was practically absent compared to MrgE or MrgF mRNA. As this result was unexpected, we tried several MrgD primers pairs to exclude the possibility of a technical problem. However, a low expression of the transcript for MrgD was consistently found. We observed circa 300 fold more mRNA expression of MrgE and 7 fold in MrgF expression compared to MasR in the SN of the same animals (Fig. 1 a).

Based on these results, we isolated mitochondria from the nigral region in the rat ventral mesencephalon (VM) and investigated the possible presence of MrgE, as an additional mitochondrial receptor that could bind Ang1-7 or other ACE2-derived peptides such as alamandine. In isolated mitochondria, we confirmed the quality of the samples with the use of specific markers such as the voltage-dependent anion channel (VDAC) for the mitochondrial fraction, and the cytosol fraction was confirmed with α-tubulin. In isolated mitochondria, we observed a much higher concentration of both ACE2 and MrgE receptors than in the whole cell homogenate (Fig. 1 b).

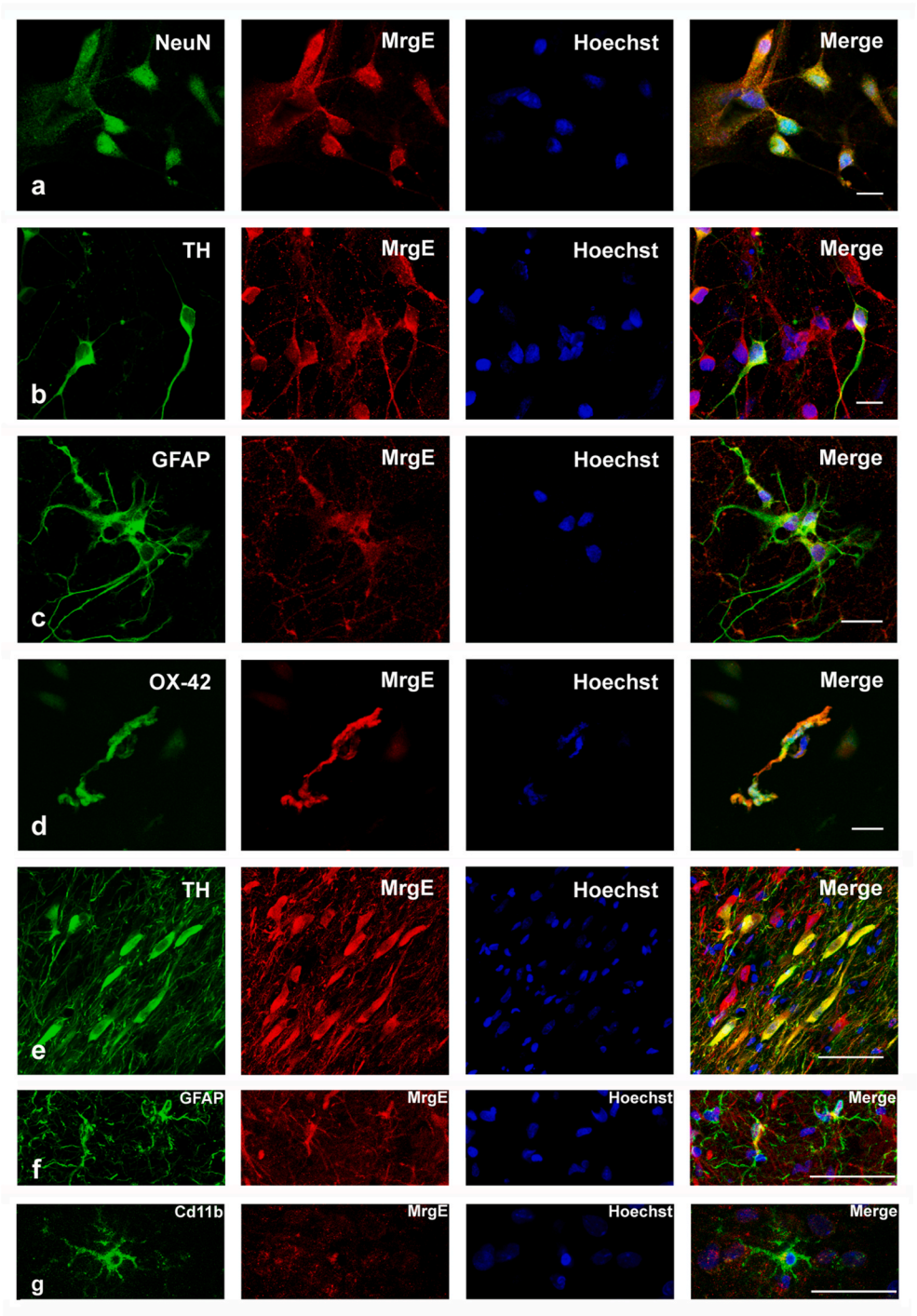

Fig. 3. Immunolabeling for MrgE in neurons and glial cells. (a–g) MrgE and Hoechst in different neuronal (NeuN as neuronal marker; TH as dopaminergic marker) and glial (GFAP as astrocytic marker, OX42 as microglial marker) cells in rat primary mesencephalic cultures (**a-d**) and tissue sections from rat substantia nigra (**e-g**). Immunolabeling for MrgE receptor was intense in neurons, and colocalized with NeuN (**a**) and TH (**b, e**). Astrocytes (**c, f**) and microglia (**d, g**) showed less intense immunolabeling. Scale bars: 25 μm (**a-d**); 50 μm (**e-g**). Abbreviations: GFAP, glial fibrillary acidic protein; MrgE, Mas-related G-protein coupled receptor member E; NeuN, Neuronal nuclear antigen; TH, tyrosine hydroxylase.

The specificity of ACE2 and MrgE antibodies was confirmed by WB analysis of HEK293 cells transfected with ACE2-GFP or MrgE-DDK. We observed a predominant immunoreactive band in transfected cells compared to control non-transfected cells at 48 post-transfection (see below) (Fig. 1 c). In addition, we confirmed the activity of the mitochondrial ACE2 using an activity assay kit (274,6 ± 23,2 mU/mg). The presence of MrgE at mitochondrial level was confirmed using confocal microscopy. In dopaminergic neuron N27 cell line, we observed co-localization of MrgE immunolabeling with the mitochondrial marker MTDR (Fig. 1 d-g).

3.2. MrgE is the most abundant MRGPR receptor subtype in rat substantia nigra, and it is also expressed in other CNS regions

After observing high levels of MrgE protein in mitochondrial preparations, we further analyzed the expression of major Mas related receptors (i.e. MrgD, MrgE and MrgF) in cell homogenates of substantia nigra (SN) and other areas of the brain. We used rat testis as a positive control tissue, as it is known that it shows a high MrgD expression and low expression of other types of Mas related receptors. We observed that MrgD mRNA was undetectable in SN relative to testis mRNA expression, confirming the specificity of the pair primers used (Fig. 2a). However, MrgE mRNA (Fig. 2b) and protein (Fig. 2e and f) expression were much

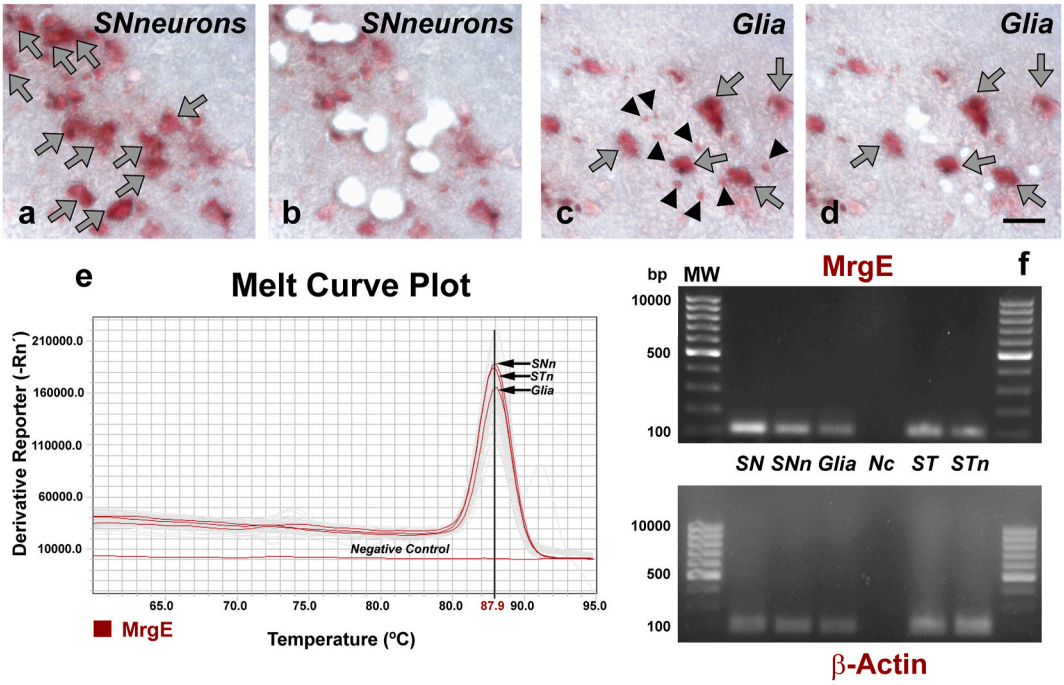

Fig. 4. Expression of MrgE in neurons or glial cells of rat substantia nigra and striatum isolated by laser microdissection and processed by RT-PCR. a–d Photomicrographs showing rat nigral sections stained with neutral red before and after laser microdissection of nigral neurons (arrows; **a, b**) or glial cells (arrowheads; **c, d**) for RT-PCR. Melting curves (**e**) and agarose gel (**f**) analysis of MrgE and the reference gene β-ACT mRNA expression in laser-micro-dissected nigral and striatal neurons and glial cells. Homogenates of substantia nigra and striatum were used as positive controls and PCR mix as negative control. Abbreviations: Nc, negative control; RT-PCR, reverse transcription-polymerase chain reaction; SN, substantia nigra homogenate; SNn, nigral neurons; Glia, glial cells; ST, striatum homogenate; STn; striatal neurons. Scale bar: 25 μm. (For interpretation of the references to colour in this figure legend, the reader is referred to the Web version of this article.)

more abundant in SN than in testis. Gene expression of MrgF subtype was not statistically different between both tissues (Fig. 2c). In addition, we confirmed the presence of MrgE mRNA (Fig. 2d) and protein (Fig. 2g and h) expression in other rat brain areas such as striatum (ST), frontal cortex (FC) and occipital cortex (OC). As in the SN region, MrgD receptors were expressed at very low level in all these brain areas compared to the same amount (μg) of tissue from testis (not shown).

3.3. *MrgE is mainly expressed in neurons and at lower levels in glial cells*

We then investigated the cell types in which MrgE was present using rat primary mesencephalic cultures (Fig. 3 a-d) and tissue sections from rat substantia nigra (Fig. 3 e-g). Immunolabeling for MrgE receptor was very intense in neurons, colocalizing with the neuronal marker NeuN (Fig. 3 a). Dopaminergic neurons, which were identified with tyrosine hydroxylase (TH), were also intensely immunolabeled for the MrgE receptor (Fig. 3b, e). Astrocytes (i.e. GFAP-positive cells; Fig. 3c, f) and microglia (OX-42 positive cells; Fig. 3d, g), were also immunolabeled for MrgE, although glial cells usually showed less intense immunolabeling. Labeling for MrgE receptor observed by confocal microscopy revealed both plasma membrane and, particularly, intracellular distribution.

Finally, laser microdissection was used to obtain isolated neurons or glial cells from the SN compacta and the striatum, which were processed by RT-PCR, and further confirmed the antibody staining by showing that the MrgE transcripts are located in the neurons and glial cells (Fig. 4).

3.4. *In the nigra of non-human primates, ACE2 and MrgE are also at high levels in the mitochondrial fraction*

Major observations in rat tissue were confirmed in non-human primates. As in rats, both ACE2 and MrgE were highly concentrated in the mitochondrial fraction relative to whole cell homogenate (Fig. 5 a, b). We confirmed the presence of ACE2 activity in monkey isolated mitochondria, which was markedly reduced by the ACE2 inhibitor DX600, revealing its functionality (Fig. 5c). In addition, tissue sections through the monkey substantia nigra showed MrgE immunolabeling, which was intense in dopaminergic neurons (i.e. TH-positive cells; Fig. 5d), but was also observed in astrocytes (GFAP-positive cells; Fig. 5e) and microglia (CD11b-positive cells; Fig. 5 f).

3.5. *MrgE binds to the ACE2-derived peptides Alamandine and Ang 1-7*

We performed fluorescence competition binding studies in MrgE-transfected HEK293 cells to address whether MrgE receptor may be labeled using FAM-conjugated alamandine (FAM-alamandine). In parallel, we also used Mas-R expressing HEK293 cells to test the binding of ligands and blockers to this receptor. In non-transfected HEK293 cells, we did not observe any significant binding of FAM-alamandine, confirming the low MrgE and Mas receptor expression in this cellular model (Fig. 6 a, f, g). However, we observed a significant binding of FAM-alamandine to both MrgE- and Mas-transfected cells. The binding of FAM-alamandine was competed by non-fluorescent alamandine and Ang 1–7 (the natural ligand of MasR), showing that both peptides are able to bind to both receptors. However, the MrgD ligand, β-alanine, only could bind to MrgE-transfected cells but not to Mas-transfected cells (Fig. 6 b, c and h-k).

Once the binding of the ligands was established, we performed binding assays with the MrgD blocker, D-Pro, and the MasR blocker, A-779. We observed that both inhibitors abolished the increase in fluorescence in MrgE- and Mas-transfected cells. This result suggests that D-Pro and A-779 can block the alamandine binding to MrgE and Mas receptors, and therefore their functional effects (Fig. 6 d, e and l, m).

3.6. *Alamandine and Angiotensin 1-7 produce an increase in cellular nitric oxide (NO) through MrgE, independently of MasR*

Due to the lack of specific ligands for MrgE receptor, we performed live-cell fluorescence time-lapse assays in HEK293 cells transfected with

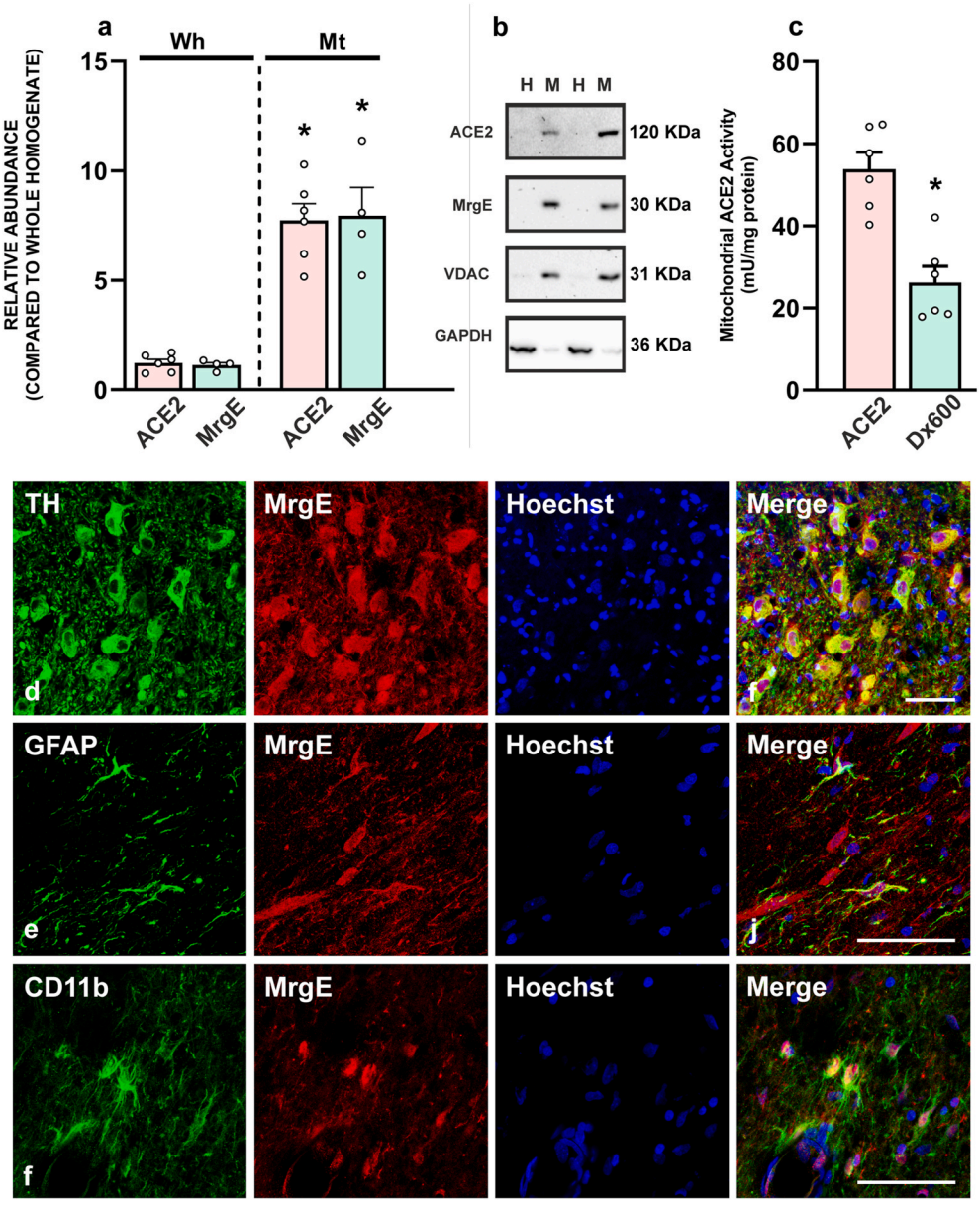

Fig. 5. ACE2 and MrgE in substantia nigra of non-human primates. (a, b) Protein in western blots from isolated mitochondria showing much higher concentration in the VDAC-positive mitochondrial fraction (Mt) than in the whole cell homogenate (Wh). **c** ACE2 activity in monkey isolated mitochondria, which was significantly reduced by the ACE2 inhibitor DX600. **(d-f)** Confocal microscopy of tissue sections through the monkey substantia nigra showing intense MrgE labelling in dopaminergic neurons (TH-positive cells, **d**) and lower levels of immunolabelling in astrocytes (GFAP-positive cells, **e**) and microglia (CD11b-positive cells, **f**). Data are presented as mean ± s.e.m. *$p < 0.05$; Student's *t*-test (MrgE) and Mann-Whitney Rank Sum Test (ACE2) (**a);** Student's *t*-test (**c**); Scale bars: 50 μm (**d-f**). Abbreviations: ACE2, Angiotensin Converting Enzyme 2; GFAP, glial fibrillary acidic protein; M or Mt, Mitochondrial fraction; H or Wh, whole homogenate; MrgE, Mas-related G-protein coupled receptor member E; TH, tyrosine hydroxylase; VDAC, Voltage-dependent anion-selective channel 1.

MrgE. To know whether the binding of alamandine and/or Ang 1–7 to MrgE-transfected cells produces functional responses, we evaluated NO release using the fluorescence DAF probe in a time period of 30 min. In the absence of treatment, no fluorescence was observed in control cells (i.e. transfected with the empty plasmid), and a very weak fluorescence was observed in MrgE transfected cells (Fig. 6 n, o and t, u). After 10 min of treatment, we observed an increase in NO-probe fluorescence in alamandine-treated MrgE transfected cells but not in control cells (Fig. 6 p, q and v, x). Moreover, treatment with Ang 1–7 also induced an increase in NO production through MrgE receptors, as revealed by the increase in green fluorescence of DAF probe in MrgE-transfected cells (Fig. 6 y, z) compared to the same treatment in control cells (Fig. 6 r, s). The NO-positive signal was observed during the 30-min measurements, slightly decreasing over the time, confirming the functionality of MrgE receptors independently of other receptors that could bind these ligands, such as MasR.

3.7. MrgE is particularly abundant in the mitochondria and regulates mitochondrial NO production

As mentioned above, we observed that MrgE receptors were enriched in the mitochondrial fraction. Consistent with this, basal NO production of N27 dopaminergic neurons, detected by the NO fluorescence probe DAF-FM, showed a marked colocalization with mitochondrial markers (Fig. 7 a-d). Furthermore, we investigated the functionality of mitochondrial MrgE receptors using isolated mitochondria from rat brain to exclude any interference of effects of cellular non-mitochondrial receptors. As in cellular assays, treatment of isolated mitochondria with alamandine produced an increase in levels of mitochondrial NO, which was inhibited by pre-incubating the mitochondria with the receptor blocker D-Pro (Fig. 7 e). We confirmed the functional effects of mitochondrial MrgE receptors using confocal microscopy of HEK293 cells transfected with MrgE receptor. We observed an increase in mitochondrial NO production in MrgE-transfected cells after 30 min of alamandine or Ang 1–7 treatment, as shown by the increase in fluorescence of DAF probes in mitochondria identified with MTDR labelling (Fig. 7 f-r). The present results suggest that mitochondrial MrgE receptors

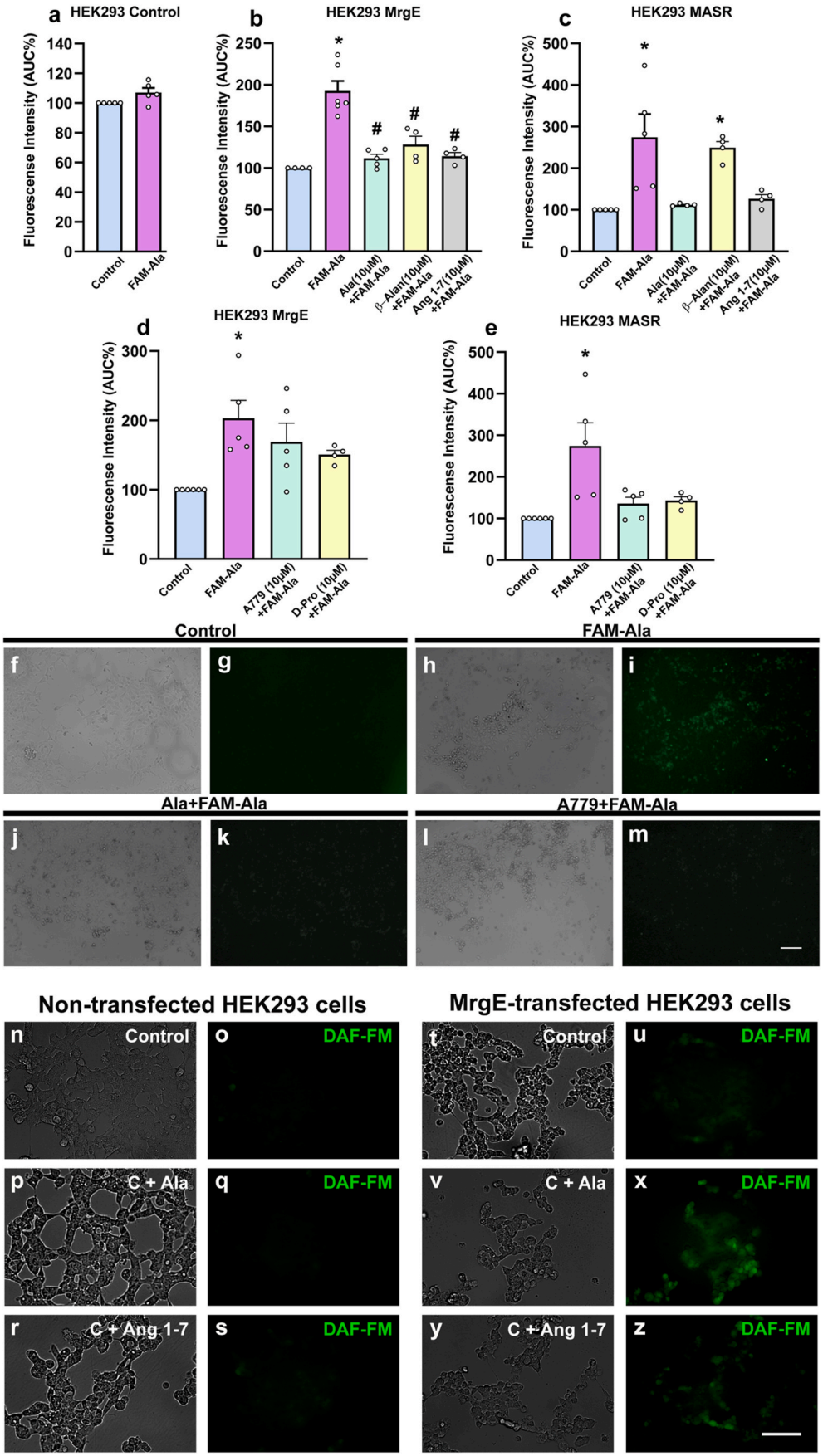

Fig. 6. Fluorescence competition binding studies (a–m) and Nitric oxide (NO) release by MrgE activation (n–z). (b, c, h, i) Fluorescence labeled (FAM)-alamandine binds to both MrgE-transfected and Mas-transfected cells. (**a, f, g)** No significant binding was observed in non-transfected control HEK293 cells. (**b, c, j, k)** The binding of FAM-alamandine was competed by non-fluorescent alamandine and Ang 1–7, showing that both peptides are able to bind both receptors; the MrgD ligand, β-alanine, only could bind MrgE-transfected cells. (**d, e, l, m)** The MrgD blocker D-Pro, and the MasR blocker A-779 abolished the increase in fluorescence (i.e. alamandine binding) in MrgE- and Mas-transfected cells. (**n, o**, **t, u)** Using a fluorescence DAF probe, NO was not observed in non MrgE transfected controls (i. e. transfected with the empty plasmid; **n, o**) and was very weak in MrgE transfected cells (**t, u**). (**p, q, v, x)** After 10 min of treatment with alamandine MrgE transfected cells (but not control cells) increased NO-probe fluorescence. (**r, s, y, z)** Treatment with Ang 1–7 also produced an increase in NO levels in MrgE-transfected cells compared to control cells. Data are presented as mean ± s.e.m. *$p < 0.05$. Mann-Whitney Rank Sum Test **(a)**; Kruskal-Wallis One Way Analysis of Variance on Ranks with Dunn's Method post hoc test **(b–e)**. Scale bar: 100 μm (**f-m**) and 90 μm (**n-z**). Abbreviations: Ala, Alamandine; Ang 1–7, Angiotensin 1-7; β-Ala, β-Alanine; D-Pro, D-Proline; DAF-FM, Diaminofluorescein-FM diacetate; FAM-alamandine, Fluorescein labeled-alamandine; MrgD, Mas-related G-protein coupled receptor member D; MrgE, Mas-related G-protein coupled receptor member E.

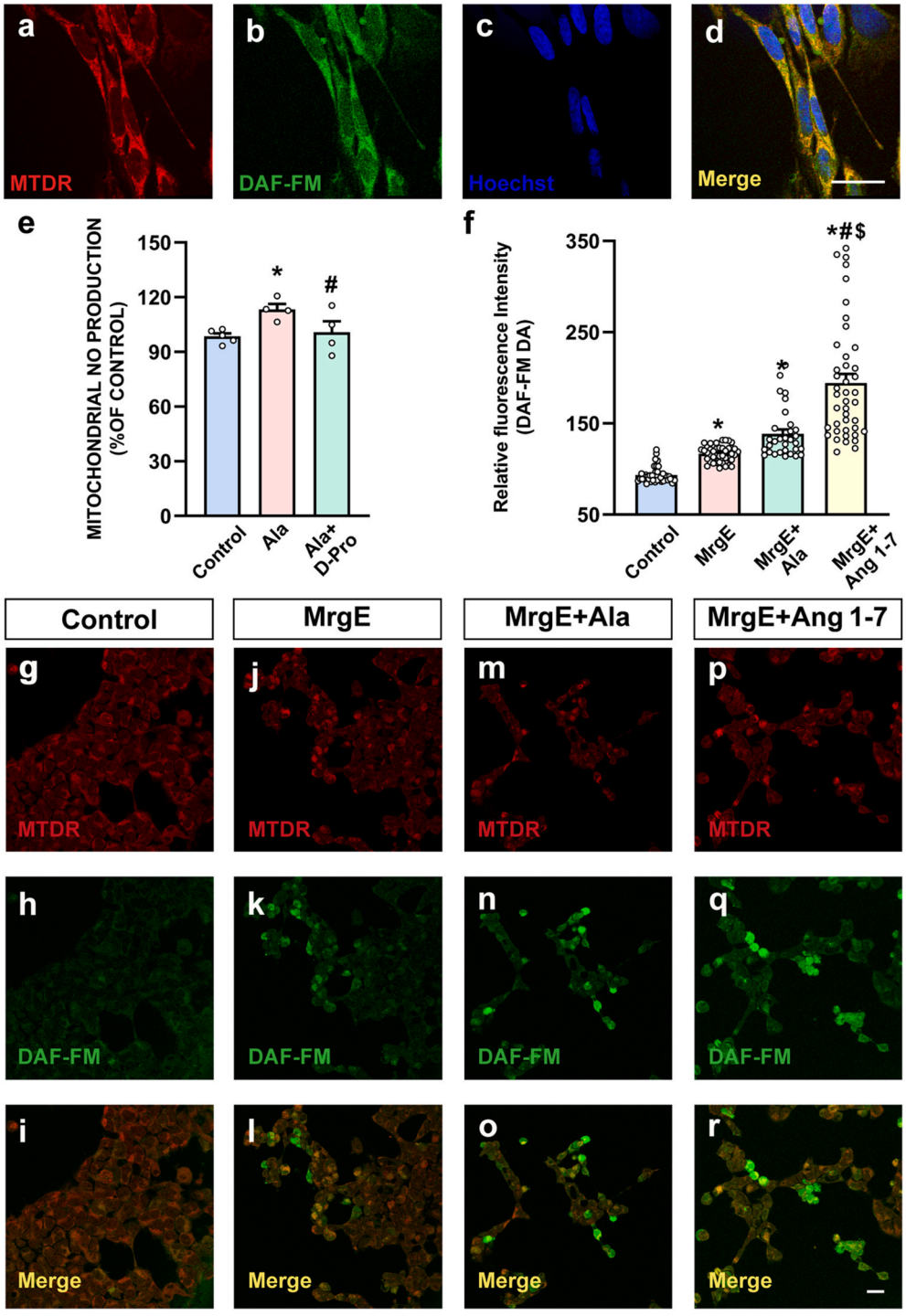

Fig. 7. Mitochondrial nitric oxide (NO) production by MrgE activation. (**a-d)** Basal mitochondrial nitric oxide (NO) colocalizing with the mitochondrial marker MTDR in N27 dopaminergic neurons. (e) Treatment of rat brain isolated mitochondria with alamandine produced an increase in levels of mitochondrial NO detected by fluorometric assay, which was inhibited by pre-incubating the mitochondria with the receptor blocker D. (**f-r)** The functional effects of mitochondrial MrgE receptors were confirmed using confocal microscopy of HEK293 cells transfected with MrgE receptor. We observed an increase in mitochondrial NO production in MrgE-transfected cells (**f, j-l**) relative to non-transfected cells (**f, g-i**), and particularly 30 min after treatment of transfected cells with alamandine (**f, m-o**), or Ang 1–7 (**f, p-r**). Data are presented as mean ± s.e.m. *p < 0.05. One Way Anova with Student-Newman-Keuls Method post hoc test (**e**); Kruskal-Wallis One Way Analysis of Variance on Ranks with Dunn's Method post hoc test (**f**). Scale bars: 25 μm (**a-d**); 10 μm (**g-r**). Abbreviations: Ala, Alamandine; Ang 1–7, Angiotensin 1-7; DAF-FM: Diaminofluorescein-FM diacetate; D-Pro, D-Proline; MrgE, Mas-related G-protein coupled receptor member E; MTDR, MitoTracker Deep Red. (For interpretation of the references to colour in this figure legend, the reader is referred to the Web version of this article.)

modulate NO production at mitochondrial level.

3.8. MrgE expression decreases with aging

In previous studies, we observed a decrease in the expression of components of the protective RAS axis, including AT2 receptors [9,24], Ang 1–7 and MasR [8] in aged animals relative to young controls. In the present work, we isolated SN from 18 to 20-month-old rats and from 2-3-month-old rats to investigate the expression of ACE2 and MrgE receptors. We observed that MrgE protein and mRNA expression decreased in substantia nigra from aged rats relative to young rats (Fig. 8 a, b). Aged animals also showed a significant decrease in ACE2 and MrgE levels in the mitochondrial fraction, and a marked increase in NOX4 levels supporting an aging-related shift of the mitochondrial RAS towards the pro-oxidative axis (Fig. 8 c-e).

4. Discussion

In the present study, we discovered that intracellular ACE2 concentrates at high levels in brain mitochondria, and that the MrgE receptor is a major target for the ACE2-related peptides Ang1-7 and alamandine, which induce mitochondrial NO production. Our previous studies in neurons [8,9] and studies in peripheral cells [25,26] have shown the presence of receptors related to both pro-oxidative and, more

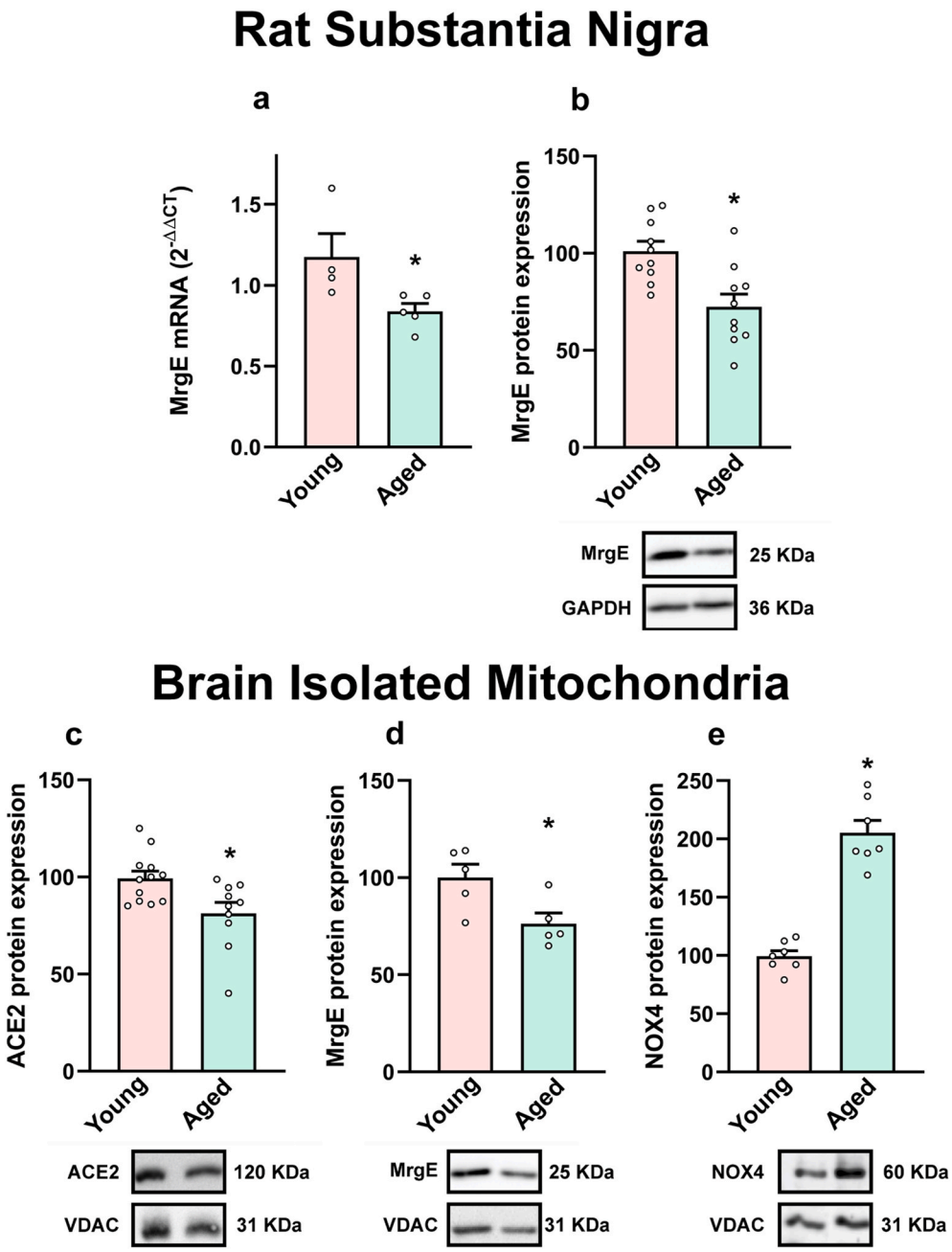

Fig. 8. Dysregulation of mitochondrial ACE2/MrgE axis by aging. (a, b) MrgE protein and mRNA expression was significantly lower in substantia nigra of aged rats relative to young rats. **(c-e)** In isolated mitochondria, aged rats also showed a significant decrease of ACE2 and MrgE levels relative to young rats, together with a marked increase in mitochondrial NOX4 levels. Data are presented as mean ± s.e.m. *$p < 0.05$, Student's *t*-test. Abbreviations: ACE2, Angiotensin Converting Enzyme 2; MrgE, Mas-related G-protein coupled receptor member E; NOX4, NADPH oxidase 4; VDAC, Voltage-dependent anion-selective channel 1.

abundantly, antioxidative RAS axes in the mitochondria. While AT1 receptors promote superoxide production via mitochondrial NOX4 activation [9], mitochondrial receptors belonging to the antioxidant axis such as AT2 receptors [9,25] and MasR [8] modulate respiration and oxidative stress by promoting NO production via mitochondrial NOS. However, mitochondrial levels of Ang 1–7 are much higher (about threefold) than mitochondrial levels of Ang II [8], and in this study we found that mitochondrial MasR are notably less abundant than MrgE receptors. Altogether suggests that the ACE2/Ang 1-7-alamandine/MrgE axis plays a major role in mitochondrial NO generation and modulation of mitochondria-derived oxidative stress, which plays a major role in dopaminergic degeneration and PD.

Consistent with this, we observed that ACE2 and MrgE are decreased in aged animals, which was also observed for other major components of the RAS antioxidative axis such as AT2 [9], Ang 1–7 and MasR [8]. A shift towards the mitochondrial pro-oxidative axis in aged animals is also supported by the present observation of significant increase in NOX4 levels in mitochondria from aged brains. This may contribute to the prooxidative proinflammatory state observed in aged brain and its vulnerability to neurodegeneration, particularly dopaminergic neuron degeneration [27]. In dopaminergic neurons, we have previously shown that the nuclear RAS [10] and the mitochondrial RAS [8,9] buffer cell oxidative stress, and particularly that derived from the paracrine RAS pro-oxidative activity. However, dysregulation of this compensatory mechanism during aging or pathological processes may lead to an excess of oxidative stress and neurodegeneration.

It is also important to highlight that ACE2 is the entry receptor of SARS-CoV and SARS-CoV-2 to invade target cells [11,28]. The effects of SARS-CoV-2 in the brain are still unclear. However, about 36 % of COVID-19 patients (45 % of severe cases) showed neurological manifestations [29], and a lesion of the brainstem neurons has been suggested to be involved in the respiratory failure in COVID-19 disease [14,30], as neuronal death has been observed in mice infected with SARS-CoV [31]. Interestingly, high affinity of coronaviruses for basal

ganglia and dopaminergic neurons has been suggested [17]. It is usually assumed that COVID-19 infection induces a decrease in levels ACE2 and ACE2 activity at the cell membrane, which results in a decrease in levels of the antioxidative Ang 1–7 and increase in levels of Ang II, leading to a shift towards the prooxidative Ang II/AT1 activity, which results in oxidative stress, inflammation and cell death. The present results open the possibility that a dysregulation of the mitochondrial ACE2/MrgE axis (i.e. the intracellular compensatory antioxidative axis) may also play a role, which should be addressed in future studies specifically designed to clarify this possibility.

Although ACE2 is the entry receptor of SARS-CoV-2, a major anti-inflammatory effect of the ACE2/Ang 1–7 axis has been shown in several organs, and particularly in the lung, which is a major target of SARS-CoV-2 and shows a high expression of ACE2 [32–34]. These two opposite effects have led to consider ACE2 as a double-edged sword for COVID-19 disease [28,35]. In recent studies, we have shown that the altered balance between both RAS axes play a major role in effects of virus/viral spike protein in human lung cells, but also in the viral spike protein internalization in cells [36,37]. However, a possible role of the mitochondrial ACE2 in virus-induced cell responses has not yet been investigated by our group or others. Several studies in lung and liver have suggested that NOX4-derived ROS may trigger the pro-inflammatory profibrotic process and that activation of the ACE2/Ang 1–7 axis may counteract this effect [38,39]. The involvement of NOX4-derived ROS has been shown because the process is blocked by NOX4 inhibitors or NOX4 siRNA, or alamandine or Ang 1–7 [38,39]. However, cell compartments involved in this NOX4 activation, and particularly the possible involvement of mitochondrial NOX4, have not been addressed. It is normally assumed that binding Ang 1–7 to cell membrane Mas receptors is responsible for the intracellular anti-oxidative responses. Previous studies have shown that viruses, including SARS-CoV viruses, modulate cell function by modifying mitochondrial processes [40,41], and that changes in mitochondrial bioenergetics play a major role both in viral replication and early cell responses to viral infection [42]. Several proteins generated from the SARS-CoV viral genome have mitochondrial targeting sequence [41,43]. Coronavirus spike proteins contain endoplasmic reticulum retrieval signals that can retrieve spike proteins to the endoplasmic reticulum [44,45]. Viral spike protein may interact with mitochondrial ACE2 via MAMs (mitochondrial associated membrane compartment) [46]. The present findings suggest that a possible role of mitochondrial ACE2 and its main target receptor MrgE should be also investigated in future studies for better comprehension of cell effects SARS-COV-2 in COVID-19.

5. Conclusions

The present study shows for the first time that MrgE receptors are predominantly expressed in mitochondria in the brain, including dopaminergic neurons. Ang 1–7 and alamandine can bind to MrgE receptors to increase NO production, which is known to counterbalance the increase in ROS at cell and mitochondrial levels. In addition, MrgE receptor expression decreases with aging, which supports the aging-related loss of the protective role of RAS. Overall, the present results suggest that MrgE, and ACE2-derived peptides Ang1-7-and alamandine play a role in mitochondrial regulation of neuronal oxidative stress, which is a major factor involved in dopaminergic neuron degeneration. Dysregulation of the mitochondrial ACE2/Ang 1-7-alamandine axis may also play role in oxidative, inflammatory and fibrotic responses related to the impairment of the ACE2 function such as that observed in COVID-19 disease. The present findings open new avenues for research on these questions.

Authors' contributions

R.V., M.A. C–B and A.L-L. performed cell cultures and in vitro experiments. A.I. R–P and P.G-G performed immunohistochemistry and in vivo experiments with rats. R.R–S, G.N. and R.F. performed binding experiments. P.G.G and J.L. L. performed experiments with monkey tissue. J.L. L-G and R. V. conceived and supervised the whole study and wrote the manuscript. All authors edited the manuscript.

Data availability

Data are available from the corresponding author upon reasonable request.

Declaration of competing interest

The authors have no competing interests related to the above-mentioned manuscript.

Acknowledgements

We thank Pilar Aldrey, Iria Novoa and Cristina Gianzo for their technical assistance. Funding: Spanish Ministry of Economy and Competitiveness (RTI2018-098830-B-I00 and RTI2018-094204-B-I00; they include EU FEDER funds). Spanish Ministry of Health (PI20/00345, RD16/0011/0016 and CIBERNED). Galician Government (XUGA, ED431C 2018/10, ED431G/05). FEDER (Regional European Development Fund).

References

[1] L.S. Capettini, F. Montecucco, F. Mach, N. Stergiopulos, R.A. Santos, R.F. da Silva, Role of renin-angiotensin system in inflammation, immunity and aging, Curr. Pharmaceut. Des. 18 (2012) 963–970.
[2] X.C. Li, D. Zhu, X. Zheng, J. Zhang, J.L. Zhuo, Intratubular and intracellular renin-angiotensin system in the kidney: a unifying perspective in blood pressure control, Clin. Sci. (Lond.) 132 (2018) 1383–1401.
[3] A. da Silva Novaes, R.S. Ribeiro, L.G. Pereira, F.T. Borges, M.A. Boim, Intracrine action of angiotensin II in mesangial cells: subcellular distribution of angiotensin II receptor subtypes AT1 and AT2, Mol. Cell. Biochem. 448 (2018) 265–274.
[4] C.E. Evans, J.S. Miners, G. Piva, C.L. Willis, D.M. Heard, E.J. Kidd, M.A. Good, P. G. Kehoe, ACE2 activation protects against cognitive decline and reduces amyloid pathology in the Tg2576 mouse model of Alzheimer's disease, Acta Neuropathol. 139 (2020) 485–502.
[5] J.L. Labandeira-Garcia, P. Garrido-Gil, J. Rodriguez-Pallares, R. Valenzuela, A. Borrajo, A.I. Rodriguez-Perez, Brain renin-angiotensin system and dopaminergic cell vulnerability, Front. Neuroanat. 8 (2014) 67.
[6] J.L. Labandeira-Garcia, J. Rodriguez-Pallares, A. Dominguez-Meijide, R. Valenzuela, B. Villar-Cheda, A.I. Rodriguez-Perez, Dopamine-angiotensin interactions in the basal ganglia and their relevance for Parkinson's disease, Mov. Disord. 28 (2013) 1337–1342.
[7] A.I. Rodriguez-Perez, D. Sucunza, M.A. Pedrosa, P. Garrido-Gil, J. Kulisevsky, J. L. Lanciego, et al., Angiotensin type 1 receptor antagonists protect against alpha-synuclein-induced neuroinflammation and dopaminergic neuron death, Neurotherapeutics 15 (2018) 1063–1081.
[8] M.A. Costa-Besada, R. Valenzuela, P. Garrido-Gil, B. Villar-Cheda, J.A. Parga, J. L. Lanciego, et al., Paracrine and intracrine angiotensin 1-7/mas receptor Axis in the substantia nigra of rodents, monkeys, and humans, Mol. Neurobiol. 55 (2018) 5847–5867.
[9] R. Valenzuela, M.A. Costa-Besada, J. Iglesias-Gonzalez, E. Perez-Costas, B. Villar-Cheda, P. Garrido-Gil, et al., Mitochondrial angiotensin receptors in dopaminergic neurons. Role in cell protection and aging-related vulnerability to neurodegeneration, Cell Death Dis. 7 (2016) e2427.
[10] B. Villar-Cheda, M.A. Costa-Besada, R. Valenzuela, E. Perez-Costas, M. Melendez-Ferro, J.L. Labandeira-Garcia, The intracellular angiotensin system buffers deleterious effects of the extracellular paracrine system, Cell Death Dis. 8 (2017), e3044.
[11] K. Kuba, Y. Imai, S. Rao, H. Gao, F. Guo, B. Guan, et al., A crucial role of angiotensin converting enzyme 2 (ACE2) in SARS coronavirus-induced lung injury, Nat. Med. 11 (2005) 875–879.
[12] R. Yan, Y. Zhang, Y. Li, L. Xia, Y. Guo, Q. Zhou, Structural basis for the recognition of SARS-CoV-2 by full-length human ACE2, Science 367 (2020) 1444–1448.
[13] A.M. Baig, A. Khaleeq, U. Ali, H. Syeda, Evidence of the COVID-19 virus targeting the CNS: tissue distribution, host-virus interaction, and proposed neurotropic mechanisms, ACS Chem. Neurosci. 11 (2020) 995–998.
[14] Y.C. Li, W.Z. Bai, T. Hashikawa, The neuroinvasive potential of SARS-CoV2 may play a role in the respiratory failure of COVID-19 patients, J. Med. Virol. 92 (2020) 552–555.
[15] J.M. Saavedra, COVID-19, angiotensin receptor blockers, and the brain, Cell. Mol. Neurobiol. 40 (2020) 667–674.
[16] A. Antonini, V. Leta, J. Teo, K.R. Chaudhuri, Outcome of Parkinson's disease patients affected by COVID-19, Mov. Disord. 35 (2020) 905–908.

[17] E. Fazzini, J. Fleming, S. Fahn, Cerebrospinal fluid antibodies to coronavirus in patients with Parkinson's disease, Mov. Disord. 7 (1992) 153–158.
[18] X. Dong, S. Han, M.J. Zylka, M.I. Simon, D.J. Anderson, A diverse family of GPCRs expressed in specific subsets of nociceptive sensory neurons, Cell 106 (2001) 619–632.
[19] P.M. Lembo, E. Grazzini, T. Groblewski, D. O'Donnell, M.O. Roy, J. Zhang, et al., Proenkephalin A gene products activate a new family of sensory neuron–specific GPCRs, Nat. Neurosci. 5 (2002) 201–209.
[20] A. Tetzner, K. Gebolys, C. Meinert, S. Klein, A. Uhlich, J. Trebicka, et al., G-Protein-Coupled receptor MrgD is a receptor for angiotensin-(1-7) involving adenylyl cyclase, cAMP, and phosphokinase A, Hypertension 68 (2016) 185–194.
[21] R.Q. Lautner, D.C. Villela, R.A. Fraga-Silva, N. Silva, T. Verano-Braga, F. Costa-Fraga, et al., Discovery and characterization of alamandine: a novel component of the renin-angiotensin system, Circ. Res. 112 (2013) 1104–1111.
[22] N.R. Sims, M.F. Anderson, Isolation of mitochondria from rat brain using Percoll density gradient centrifugation, Nat. Protoc. 3 (2008) 1228–1239.
[23] P. Garrido-Gil, P. Fernandez-Rodríguez, J. Rodríguez-Pallares, J.L. Labandeira-Garcia, Laser capture microdissection protocol for gene expression analysis in the brain, Histochem. Cell Biol. 148 (2017) 299–311.
[24] A.I. Rodriguez-Perez, P. Garrido-Gil, M.A. Pedrosa, M. Garcia-Garrote, R. Valenzuela, G. Navarro, et al., Angiotensin type 2 receptors: role in aging and neuroinflammation in the substantia nigra, Brain Behav. Immun. 87 (2020) 256–271.
[25] P.M. Abadir, D.B. Foster, M. Crow, C.A. Cooke, J.J. Rucker, A. Jain, et al., Identification and characterization of a functional mitochondrial angiotensin system, Proc. Natl. Acad. Sci. U. S. A. 108 (2011) 14849–14854.
[26] B.A. Wilson, M. Nautiyal, T.M. Gwathmey, J.C. Rose, M.C. Chappell, Evidence for a mitochondrial angiotensin-(1-7) system in the kidney, Am. J. Physiol. Ren. Physiol. 310 (2016) F637–F645.
[27] B. Villar-Cheda, R. Valenzuela, A.I. Rodriguez-Perez, M.J. Guerra, J.L. Labandeira-Garcia, Aging-related changes in the nigral angiotensin system enhances proinflammatory and pro-oxidative markers and 6-OHDA-induced dopaminergic degeneration, Neurobiol. Aging 33 (2012) 204, e1-11.
[28] T. Yan, R. Xiao, G. Lin, Angiotensin-converting enzyme 2 in severe acute respiratory syndrome coronavirus and SARS-CoV-2: a double-edged sword? Faseb. J. 34 (2020) 6017–6026.
[29] L. Mao, H. Jin, M. Wang, Y. Hu, S. Chen, Q. He, et al., Neurologic manifestations of hospitalized patients with coronavirus disease 2019 in wuhan, China, JAMA Neurol 77 (2020) 683–690.
[30] Jr, P.B. McCray, L. Pewe, C. Wohlford-Lenane, M. Hickey, L. Manzel, L. Shi, et al., Lethal infection of K18-hACE2 mice infected with severe acute respiratory syndrome coronavirus, J. Virol. 81 (2007) 813–821.
[31] J. Netland, D.K. Meyerholz, S. Moore, M. Cassell, S. Perlman, Severe acute respiratory syndrome coronavirus infection causes neuronal death in the absence of encephalitis in mice transgenic for human ACE2, J. Virol. 82 (2008) 7264–7275.
[32] I. Hamming, W. Timens, M.L. Bulthuis, A.T. Lely, G. Navis, H. van Goor, Tissue distribution of ACE2 protein, the functional receptor for SARS coronavirus. A first step in understanding SARS pathogenesis, J. Pathol. 203 (2004) 631–637.
[33] H. Zhang, J.M. Penninger, Y. Li, N. Zhong, A.S. Slutsky, Angiotensin-converting enzyme 2 (ACE2) as a SARS-CoV-2 receptor: molecular mechanisms and potential therapeutic target, Intensive Care Med. 46 (2020) 586–590.
[34] N. Klein, F. Gembardt, S. Supe, S.M. Kaestle, H. Nickles, L. Erfinanda, et al., Angiotensin-(1-7) protects from experimental acute lung injury, Crit. Care Med. 41 (2013) e334–343.
[35] K. Wang, M. Gheblawi, G.Y. Oudit, Angiotensin converting enzyme 2: a double-edged sword, Circulation 142 (2020) 426–428.
[36] M.A. Pedrosa, R. Valenzuela, P. Garrido-Gil, C.M. Labandeira, G. Navarro, R. Franco, J.L. Labandeira-Garcia, A.I. Rodriguez-Perez, Experimental data using candesartan and captopril indicate no double-edged sword effect in COVID-19, Clin. Sci. (Lond.) 135 (2021) 465–481.
[37] R. Valenzuela, M.A. Pedrosa, P. Garrido-Gil, C.M. Labandeira, G. Navarro, R. Franco, A.I. Rodriguez-Perez, J.L. Labandeira-Garcia, Interactions between ibuprofen, ACE2, renin-angiotensin system and spike protein in the lung. Implications for COVID-19, Clin. Transl. Med. 11 (4) (2021) e371.
[38] Y. Huang, Y. Li, A. Lou, G.Z. Wang, Y. Hu, Y. Zhang, et al., Alamandine attenuates hepatic fibrosis by regulating autophagy induced by NOX4-dependent ROS, Clin. Sci. (Lond.) 134 (2020) 853–869.
[39] Y. Meng, T. Li, G.S. Zhou, Y. Chen, C.H. Yu, M.X. Pang, et al., The angiotensin-converting enzyme 2/angiotensin (1-7)/Mas axis protects against lung fibroblast migration and lung fibrosis by inhibiting the NOX4-derived ROS-mediated RhoA/Rho kinase pathway, Antioxidants Redox Signal. 22 (2015) 241–258.
[40] P. Boya, A.L. Pauleau, D. Poncet, R.A. Gonzalez-Polo, N. Zamzami, G. Kroemer, Viral proteins targeting mitochondria: controlling cell death, Biochim. Biophys. Acta 1659 (2004) 178–189.
[41] X. Yuan, Y. Shan, Z. Yao, J. Li, Z. Zhao, J. Chen J, et al., Mitochondrial location of severe acute respiratory syndrome coronavirus 3b protein, Mol. Cell. 21 (2006) 186–191.
[42] L. Silva da Costa, A.P. Pereira da Silva, A.T. Da Poian, T. El-Bacha, Mitochondrial bioenergetic alterations in mouse neuroblastoma cells infected with Sindbis virus: implications to viral replication and neuronal death, PloS One 7 (2012), e33871.
[43] K.K. Singh, G. Chaubey, J.Y. Chen, P. Suravajhala, Decoding SARS-CoV-2 hijacking of host mitochondria in COVID-19 pathogenesis, Am. J. Physiol. Cell Physiol. 319 (2020) C258–C267.
[44] E. Lontok, E. Corse, C. E Machamer, Intracellular targeting signals contribute to localization of coronavirus spike proteins near the virus assembly site, J. Virol. 78 (2004) 5913–5922.
[45] J. Sadasivan, M. Singh, J.D. Sarma, Cytoplasmic tail of coronavirus spike protein has intracellular targeting signals, J. Biosci. 42 (2017) 231–244.
[46] C.D. Williamson, A.M. Colberg-Poley, Access of viral proteins to mitochondria via mitochondria-associated membranes, Rev. Med. Virol. 19 (2009) 147–164.